Cerebral Cortex December 2008;18:2941–2951
doi:10.1093/cercor/bhn054
Advance Access publication April 18, 2008

Auditory, Somatosensory, and Multisensory Insular Cortex in the Rat

Krista M. Rodgers, Alexander M. Benison, Andrea Klein and Daniel S. Barth

Department of Psychology, University of Colorado, Boulder, CO 80309-0345, USA

Compared with other areas of the forebrain, the function of insular cortex is poorly understood. This study examined the unisensory and multisensory function of the rat insula using high-resolution, whole-hemisphere, epipial evoked potential mapping. We found the posterior insula to contain distinct auditory and somatotopically organized somatosensory fields with an interposed and overlapping region capable of integrating these sensory modalities. Unisensory and multisensory responses were uninfluenced by complete lesioning of primary and secondary auditory and somatosensory cortices, suggesting a high degree of parallel afferent input from the thalamus. In light of the established connections of the posterior insula with the amygdala, we propose that integration of auditory and somatosensory modalities reported here may play a role in auditory fear conditioning.

Keywords: AEP, evoked potentials, PV, secondary, SEP

Introduction

Despite advances made in our understanding of neocortical function, the function of the insula remains obscure (Flynn 1999). Unlike gyrencephalic brain, where the insula are buried beneath the operculum, the lisencephalic brain of the rat has an insular region located on the lateral surface of the cerebral hemisphere, providing a far more accessible preparation for study. Cytoarchitectural, hodological, and functional studies of the rat insular region have yielded a variety of proposed areal parcelations (Deacon et al. 1983; Guldin and Markowitsch 1983; Shi and Cassell 1997; McDonald 1998; Shi and Cassell 1998; McDonald et al. 1999; Aleksandrov and Fedorova 2003). However, a common agreement among these studies is that the insula straddles the rhinal sulcus and may be divided into anterior and posterior regions (McDonald et al. 1999). Anterior insula is considered to be involved in gustatory and visceral functions (Kosar et al. 1986a, 1986b; Cechetto and Saper 1987; Fabri and Burton 1991a, 1991b; Shi and Cassell 1997; McDonald 1998; McDonald et al. 1999). Based on anatomical (Akers and Killackey 1978; Guldin and Markowitsch 1983; Fabri and Burton 1991a, 1991b; Paperna and Makach 1991; McIntyre et al. 1996; McDonald 1998; Shi and Cassell 1998; McDonald et al. 1999) and functional (Ito 1998; Remple et al. 2003; Benison et al. 2007) evidence, posterior insula is thought to be involved in somesthesis.

Although the somatosensory function of the posterior insula has been established, there is limited evidence that the insula may also participate in auditory processing (Bamiou et al. 2003). In monkeys and rats, the posterior insula receive thalamic projections from the medial geniculate (MG) nucleus (Burton and Jones 1976; Krettek and Price 1977; Guldin and Markowitsch 1983) and intracortical projections from auditory cortex (Guldin and Markowitsch 1983; Mesulam and Mufson 1985; Paperna and Makach 1991; Kimura et al. 2007). Recent imaging studies in humans have also revealed auditory activation of the insula (Bamiou et al. 2003). Interestingly, in the rat, intracortical auditory projections target insular areas quite anterior to any known field of primary or secondary auditory cortex (Kimura et al. 2007; Polley et al. 2007), suggesting that the insula may have a complete auditory field that is anatomically and functionally distinct from auditory temporal cortex.

The goals of the present study were to examine the functional anatomy of rat insular cortex, using high-resolution, whole-hemisphere field potential mapping, to 1) determine if there is an auditory area of the insula that is distinct from primary and secondary auditory cortex, 2) establish areal boundaries between somatosensory insula and secondary auditory cortex as well as putative auditory insula, 3) explore the possibility that rat insula may perform multisensory (auditory/somatosensory) integration, as suggested by fMRI studies in humans (Downar et al. 2000), and 4) use targeted lesioning (based on field potential mapping) of primary and secondary somatosensory and auditory cortex to determine the extent to which sensory activation of the insula is based on intracortical versus thalamocortical pathways.

Materials and Methods

Animals and Surgery

All procedures were performed in accordance with University of Colorado Institutional Animal Care and Use Committee guidelines for the humane use of laboratory animals in biological research. A total of 9 adult male Sprague–Dawley rats (300–400 g) were anesthetized to surgical levels using an intraperitoneal injection of urethane (1.25 g/kg body weight), placed on a regulated heating pad, and maintained with subsequent injections throughout the experiment so that the eye blink reflex could be barely elicited. A unilateral craniectomy was performed over the left hemisphere extending from bregma to 3 mm rostral of lambda and from the mid-sagittal suture past the lateral aspect of the temporal bone, exposing a maximal area of the surgically accessible hemisphere. The dura was reflected and the exposed cortex regularly doused with Ringer Solution containing: NaCl 135 mM; KCl 3 mM; MgCl 2 mM; and CaCl 2 mM—pH 7.4 at 37 °C. Animals were euthanized by anesthesia overdose without regaining consciousness at the conclusion of the experiment.

Stimulation

Somatosensory responses were evoked by electrical stimulation of the forepaw, hindpaw, and mid-trunk that were shaved and coated with conductive jelly. A bipolar electrode (500 μm tips; 1 mm separation) attached to a constant current source delivered biphasic current pulses (1 ms) to the exposed skin. Auditory click stimuli (0.1 ms monophasic

pulses) were delivered using a high frequency piezoelectric speaker placed approximately 15 cm lateral to the contralateral ear. During auditory and somatosensory stimulation, intensities were adjusted to the lowest level yielding a stable evoked potential. Adequate auditory stimuli were approximately 30-dB sound pressure level (SPL) at 15 cm, and thus innocuous. In contrast, somatosensory stimuli required to evoke reliable potentials from the insula were in the range of 1.0–2.0 mA, exceeding the typical 0.5 mA used as noxious foot shock stimuli in fear conditioning studies (Lanuza et al. 2004). In 2 nonsurgical animals, this current level resulted in slight twitching of the forepaw or hindpaw under anesthesia but vigorous withdrawal reflexes without anesthesia, suggestive of a noxious stimulation. Whisker stimulation was provided by 0.1 ms pulses delivered to a solenoid with attached 3 cm armature constructed from hypodermic tubing. Whisker displacements were approximately 0.5 mm on the rostro-caudal axis.

Evoked Potential Recording

Epipial maps of unimodal auditory and somatosensory evoked potentials (AEP and SEP, respectively), and multimodal auditory/somatosensory evoked potentials (ASEP), were recorded using a flat multielectrode array consisting of 256 Ag wires in a 16 × 16 grid (tip diameter: ~100 μm; interelectrode spacing: 500 μm) covering a 7.5 × 7.5 mm area of the left hemisphere in a single placement (Benison et al. 2007). The array was pressed against the cortex with sufficient force to establish contact of all electrodes. The required pressure had no effect on evoked potential amplitude, poststimulus latency, or morphology when compared with potentials recorded previously with more lightly placed small arrays. Recordings were referenced to a Ag/AgCl ball electrode secured over the contralateral frontal bone, and were simultaneously amplified (2000×; NerveAmp, Center for Neural Recording, Washington State University, Pullman, WA), analog filtered (band-pass cut-off = –6 dB at 0.1 to 3000 Hz, roll-off = 5 db/octave) and digitized at 10 kHz. Evoked potentials were averaged over 64 stimulus presentations. The array was consistently aligned across animals using potentials recorded in the posteromedial barrel subfield evoked by separately stimulating the rostral and caudal whisker in the middle row (C5 and C1) and the dorsal and ventral whisker in the middle arc (A3 and E3).

Radio Frequency Lesioning

In 5 of the animals, selective lesioning of the forepaw representation of primary and secondary somatosensory and auditory cortex were performed by 1st identifying areas of maximum responsiveness with the 256 electrode recording array. The array was removed and replaced with a transparent scaled template, which allowed verification of the specific electrode locations in relation to underlying vasculature prior to lesioning. All lesions were made unilaterally with a stainless steel electrode (diameter, 250 μm) by passing an anodal current of ~3 mA with a lesion generator system (Radionics model RFG-4A Research RF, Burlington, MA). The tissue temperature at the tip of the electrode was set to 75 °C for 1 minute. At a given site, lesions were made at electrode depths of 1.5, 1.0, and 0.5 mm. This resulted in a structural lesion area of approximately 2 mm diameter. However, functional suppression of evoked potentials extended beyond this to approximately 3 mm diameter. After single lesions were placed in the center of a responsive area, the recording array was replaced and residual evoked responses used to guide subsequent lesions. This procedure was repeated until all responses in primary and secondary cortex were eliminated. The same 5 animals tested with lesions were also evaluated for multisensory interactions before and after lesioning.

Data Collection and Analysis

Regions of auditory and somatosensory cortex were estimated from interpolated (bicubic spline) maps of evoked potential amplitude across the recording array at select poststimulus latencies. The initial positive component (P1) of the evoked potential complex occurred at the shortest poststimulus latency, and the center of its mapped amplitude peak was visually identified and used to locate regions of responsive cortex (an example of the mapping procedure is shown in Fig. 1). Cortical areas uniquely responding to multisensory stimulation were evaluated by subtracting the multimodal ASEP from a linear model computed from the sum of the unimodal AEP and SEP. This model was subtracted from the ASEP, and the root mean squared (RMS) power of the resulting difference waveform computed at each electrode site and mapped across electrodes to identify the locus and extent of multisensory cortex. This procedure was based on the assumption that, unlike linearly summed volume currents, cortical areas where multisensory interactions occur will typically produce responses that are sub- or supra-additive and of different poststimulus latency than that predicted from the linear model (Dehner et al. 2004; Rowland et al. 2007; Stanford and Stein 2007). Differences in the poststimulus latencies of the ASEP and the linear model at a given electrode site were derived from the time lag at which the cross-correlation function between the 2 waveforms was maximum. Locations of auditory, somatosensory, and multisensory responsive regions were digitally logged, and their interareal differences, positions in relation to bregma, as well as response amplitudes, poststimulus latencies, and RMS power (in the case of multisensory response) were reported as the mean and standard error of the mean. Significant differences between cortical loci as well as response parameters were evaluated using t-tests with significance set to $P \leqslant 0.05$.

Results

Auditory and Somatosensory Fields in the Insula.

Figure 1*A* shows the most lateral placement of the epipial recording array in a single animal, applied with sufficient pressure to flatten the underlying 7.5 × 7.5 mm cortex of the left hemisphere. Photographic record of the upper border of the array in relation to bregma and the superior cerebral veins (Fig. 1*A*; arrowheads) permitted subsequent replacement of the array with a transparent scaled template to establish electrode locations in relation to underlying vascular patterns (Fig. 1*B*). Thus, 256 AEPs are plotted in Figure 1*B*, reflecting the auditory response at each electrode within the array. AEPs were largest in a caudal region of the array approximately 4 mm caudal to bregma, 1.5 mm lateral to the middle cerebral artery and 3.5 mm medial to the rhinal vein (Fig. 1*B*; black traces), corresponding approximately to the locus of the anterior auditory field (AAF; Polley et al. 2007). The AEP amplitude fell sharply at the rostral border of AAF, separating AAF from a rostral island of responsiveness of approximately 2 mm diameter (Fig. 1*B*; blue traces) that we have labeled the insular auditory field (IAF) due to its close proximity to the rhinal vein (<1.0 mm medial) and extreme rostral locus (1 mm caudal to bregma). The AEP complex in both IAF and AAF consisted of a typical biphasic (positive/negative) sharp wave (Fig. 1*B*; insert) labeled P1 and N1 to reflect the sequence and polarity of the amplitude peaks. Across animals, the P1 and N1 amplitudes in IAF (Fig. 1*B* insert; blowup of blue trace circled in "a"; 0.4 ± 0.03 and –0.8 ± 0.05 mV; $N = 9$) were significantly lower (1.1 ± 0.05 and 2.2 ± 0.14 mV; $P < 0.01$; $N = 9$) than those of AAF (Fig. 1*B* insert; blowup of black trace circled in "b"; 1.5 ± 0.06 and –2.8 ± 0.16 mV; $N = 9$). Interestingly, poststimulus latencies of the P1 and N1 peaks in IAF (18.4 ± 0.02 and 26.7 ± 0.03 ms; $N = 9$) were also significantly shorter (1.1 ± 0.01 and 1.2 ± 0.02 ms; $P < 0.01$ and 0.02; $N = 9$) than latencies for the same components in AAF (19.2 ± 0.02 and 27.6 ± 0.02 ms), suggesting that IAF did not rely on intracortical projections from AAF for access to auditory input. To provide a more accurate measure of the locus, areal extent, and separation of IAF and AAF, topographical maps, reflecting the normalized amplitude distribution at the poststimulus latency of the P1 (the earliest and therefore most focal

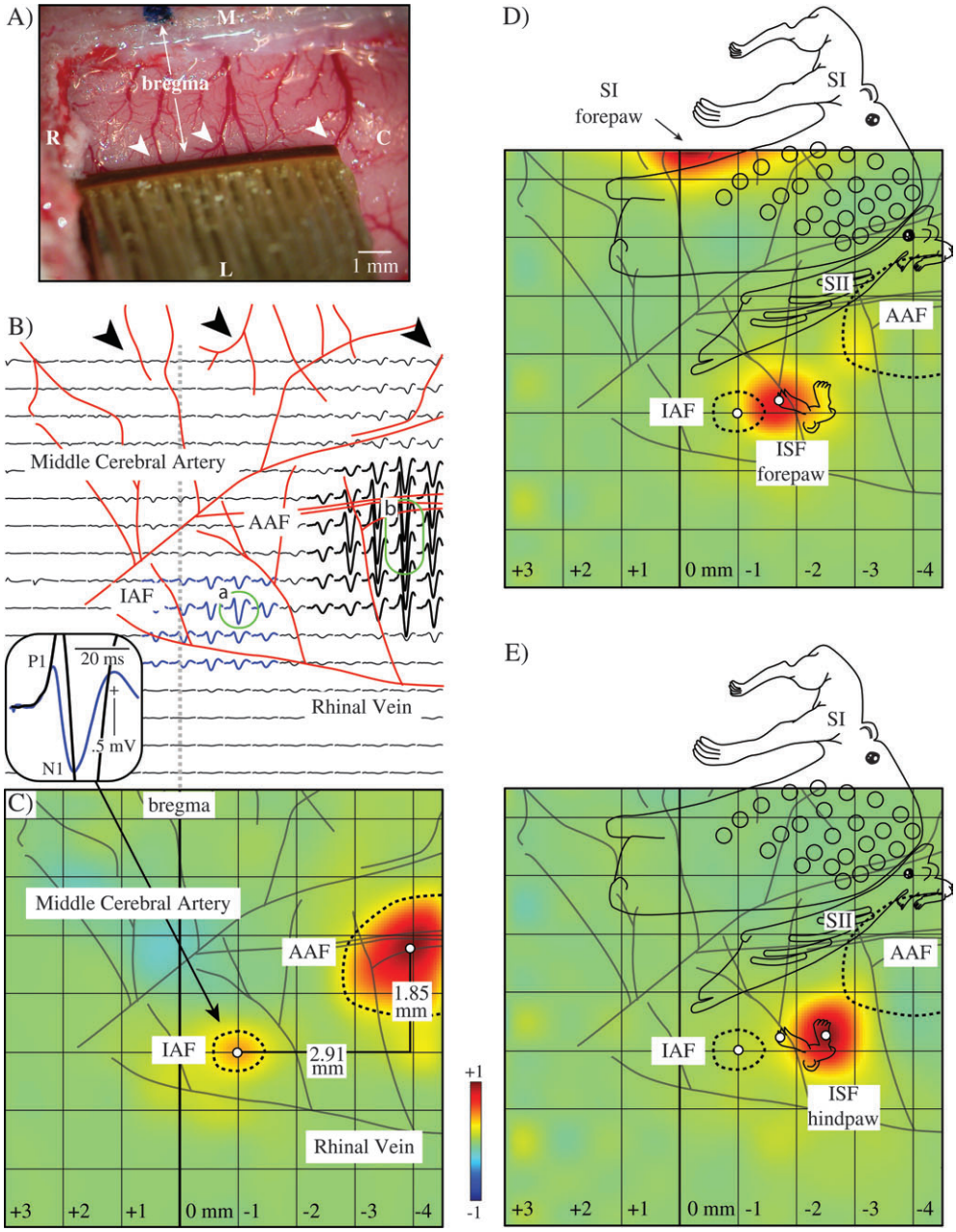

Figure 1. Auditory and somatosensory fields in the insula. (*A*) Photographic record showing the most lateral placement of the epipial recording array in relation to bregma and the superior cerebral veins (arrowheads). (*B*) A transparent scaled template of the array was used to establish electrode locations in relation to underlying vasculature. AEP were then plotted in register with these electrode locations. Blue traces indicate responses in the IAF and black traces in the AAF. Representative AEPs (green circled traces) in both IAF (*a*) and AAF (*b*) consisted of a typical biphasic, positive/negative sharp wave (insert; P1/N1). The AEP in IAF was of smaller amplitude and shorter poststimulus latency than that recorded in AAF. (*C*) Topographical map reflecting the normalized amplitude distribution at the poststimulus latency of the P1 (earliest component, see insert). Note here that IAF was 1.85 mm lateral and 2.91 mm caudal to the center of AAF (50% amplitude iso-potential contours shown as dashed lines). (*D*) Electrical stimulation of forepaw yielded a focal SEP response that partially overlapped IAF, but was centered more caudally and is labeled the ISF (forepaw). (*E*) Electrical stimulation of hindpaw evoked an SEP that was shifted more caudal than the forepaw response (ISF hindpaw). For anatomical reference, a template of somatosensory representations derived from a more extensive mapping study of primary, secondary, and the lateral insular somatosensory cortex (Benison et al. 2007) is superimposed on the maps of (*D*) and (*E*) and subsequent figures.

component), were computed (Fig. 1*C*). In the example of Figure 1, the center of IAF was 2.91 mm rostral and 1.85 mm lateral to the center of AAF. The borders of both areas are demarked with a dashed line representing the iso-potential of 50% amplitude. Across animals, IAF was 2.7 ± 0.02 mm ($P < 0.01$; $N = 9$) rostral and 1.5 ± 0.03 mm ($P < 0.01$; $N = 9$) lateral to AAF.

Note here and elsewhere that the standard error of localizations based on field potential maps is quite small, under 100 μm. This has been observed in previous studies using these methods (Rodgers et al. 2006; Benison et al. 2007) and is due to 5 factors that should be described here because all subsequent results rely on this spatial resolution. First, recordings were performed epipially, eliminating smearing effects of the skull

and dura mater. Second, only cortical activity at the earliest positive deflection of the evoked potential is mapped, reflecting the most focal signal before subsequent intracortical spread. Third, these maps are of averaged (N = 64) trials, greatly decreasing their variance. Fourth, distances between areas (i.e. IAF and AAF in this example) are computed in relative coordinates, eliminating slight errors due to variation in array placement between animals. Finally, and perhaps most important, whereas the spacing of the electrodes in the array is 0.5 mm, the resolution is much better than this because bicubic spline interpolated maps used here take advantage of the 2 dimensional spatial gradient of potential amplitude, a process similar to triangulating on a point from several widely spaced detectors, and providing an accuracy much better than the spacing of the detectors.

Electrical stimulation of the forepaw yielded a focal SEP response (Fig. 1*D*; insular somatosensory field [ISF] forepaw) that partially overlapped the IAF but was centered 0.9 ± 0.02 mm (P < 0.01; N = 9) caudally in the parietal ventral (PV) area (Krubitzer et al. 1986; Fabri and Burton 1991a; Benison et al. 2007). Similarly, hindpaw stimulation evoked an SEP that was shifted more caudal (0.7 ± 0.01 mm; P < 0.01; N = 9) than the forepaw response, at a locus 1.5 ± 0.02 mm (P < 0.02; N = 9) caudal to the IAF (Fig. 1*E*; ISF hindpaw). Stimulation of the mid-trunk (not shown) also evoked a response positioned lateral to the forepaw and hindpaw representations (0.3 ± 0.05 and 0.4 ± 0.07 mm; P < 0.04 and 0.05; N = 9). Somatosensory responses thus formed an inverted representation of the body that replicated more extensive mapping of the PV in a previous study (Benison et al. 2007). A template of somatosensory representations derived from this previous work for primary (SI) and secondary (SII) somatosensory cortex, and PV, was therefore superimposed on the maps of Figure 1*D*,*E* and subsequent figures for anatomical reference. As in previous work (Benison et al. 2007) responses in SII to stimulation of the distal extremities were smaller than in ISF. Maps of Figure 1*D*,*E* were chosen at latencies when the ISF was largest, not the smaller response in SII. This, in combination with the fact that the maps were normalized to the much larger SI responses, attenuated the forepaw and hindpaw responses in SII (however, see Fig. 2*A*; bottom plate; and Fig. 2*E*; top plate for forepaw responses in SII). Given the close proximity of somatosensory responses in PV to the IAF and to the rhinal vein, and the location of both of these regions within the insula according to numerous areal parcellation schemes (see Discussion) we refer to this area as the ISF as opposed to PV. As in a previous study of this region (Benison et al. 2007), representations in ISF were dominated by the distal extremities and showed markedly attenuated responses to the pinna and none to mechanical vibrissa displacements. Poststimulus latencies of the P1 of the SEP in ISF for forepaw, hindpaw and mid-trunk stimulation (19.8 ± 0.19, 23.1 ± 0.29 and 23.5 ± 0.71 ms; N= 9) compared with similar responses in SI (18.2 ± 0.23, 22.4 ± 0.15 and 20.3 ± 0.43 ms; N = 9) were significantly delayed (1.6 ± 0.13, 0.4 ± 0.06 and 1.8 ± 0.29 ms; P < 0.01; N = 9). Latencies of the N1 in ISF for forepaw, hindpaw and mid-trunk stimulation (38.6 ± 0.89, 42.8 ± 0.21 and 44.3 ± .0.12 ms; N= 9) compared with SI (29.1 ± 0.48, 32.6 ± 0.66 and 29.8 ± 0.10 ms; N= 9) were also delayed (9.4 ± 0.72, 5.8 ± 1.7 and 8.3 ± 1.9 ms; P < 0.01; N= 9). Thus unlike IAF, where insular response latencies were earlier than primary cortex, those in ISF were later, suggesting a possible contribution of intracortical projections from SI to ISF.

Multisensory Interactions

The close proximity of IAF to ISF, and the partial overlap of auditory and somatosensory responses, raised the question of whether there was multisensory interaction within the insula. We therefore measured whether regions of the insula responded uniquely to simultaneous combined auditory and forepaw stimulation with multisensory ASEPs that significantly differed from what might be anticipated from the linear sum of the AEP and SEP when recorded separately (AEP + SEP or ASEPmod). The justification for examining nonlinear multisensory responses was that if auditory and somatosensory specific cells were simply interdigitated but did not interact, or if the AEP and SEP overlapped only due to volume conducted field potentials from IAF and ISF respectively, the ASEP would exactly equal the ASEPmod. However, if the ASEP amplitude was greater (supra-additive) or less (subadditive) than the ASEPmod, or its poststimulus latency differed, this would be a clear indication of increased or decreased activation due to excitatory or

Figure 2. Unisensory and multisensory responses in intact and lesioned preparations (*A*) Somatosensory map of the forepaw representations of both SI and ISF in a single animal (top map). The SEP from an electrode site just rostral to ISF and caudal to IAF (filled white dot on map) is enlarged (middle black trace). A map of the grand averaged SEP (N = 9) to forepaw stimulation (bottom map). A weak response in the forepaw representation of SII marked with an arrow. (*B*) Auditory map of AAF and IAF in the same animal (top map) and averaged across animals (bottom map). The AEP (middle blue trace) was smaller than the SEP (black trace) at the chosen recording site. The red trace represents a linear model (ASEPmod) computed by adding the unimodal AEP and SEP. (*C*) Simultaneous auditory and somatosensory (forepaw) stimulation, at the same intensities as used for unisensory responses, yielded a multisensory response pattern reflecting the spatial distribution of the single (top map) and grand averaged (bottom map) ASEP. The ASEP (middle black trace) was of lower amplitude and shorter poststimulus latency than the ASEPmod (middle red trace), indicating multisensory interactions between IAF and ISF during combined stimulation. (*D*) The magnitude of multisensory interaction multisensory interaction was quantified by subtracting the ASEPmod from the ASEP, resulting in a difference waveform (middle black trace). The overall amplitude of the difference waveform was computed as the RMS power. The power map for a single animal (top map; note that blue represents maximum power) indicated substantial multisensory responsiveness overlapping the forepaw representation of ISF as well as the interposed region between ISF and IAF (*a*). Smaller multisensory regions were also apparent at the rostral (*b*) and medial (*c*) borders of AAF. The distribution of multisensory interaction, when averaged across animals (bottom map) was wider, covering both IAF and ISF, interposed cortex, and the rostral and medial areas of AAF. Electrode sites where interactions reached significance (P < 0.05) are depicted as white dots. (*E*) An example of the forepaw response in a single animal (top map) prior to lesioning. Such maps were used to guide radio frequency lesioning, 1st in the center of the SI forepaw representation (bottom map; filled white circle shows the approximate location and extent of the 1st lesion) and then adjacent spots (empty red circles) until the SEP in the forepaw representations of both SI and SII were completely eliminated. Postlesion, the response in ISF (insert; red trace) was nearly unchanged in morphology, amplitude or poststimulus latency compared with the prelesion response (insert; black trace). (*F*) Pre- (top map) and post- (bottom map) lesion AEPs also demonstrate persistent responses in IAF that were unchanged before (insert; black trace) and after (insert; red trace) complete lesioning of primary and secondary auditory cortex. (*G*) In this same animal, the spatial distribution (top map) and waveform characteristics (insert) of the multisensory ASEP appeared unchanged before (black trace) and after (red trace) complete lesioning of primary and secondary auditory and somatosensory cortex. Pre- and postlesion difference waveforms (bottom map; insert) were similarly unaffected by the lesion, and multisensory responsiveness remained in regions in and about IAF and ISF. Postlesion multisensory responsiveness was significant in this region across animals (white dots).

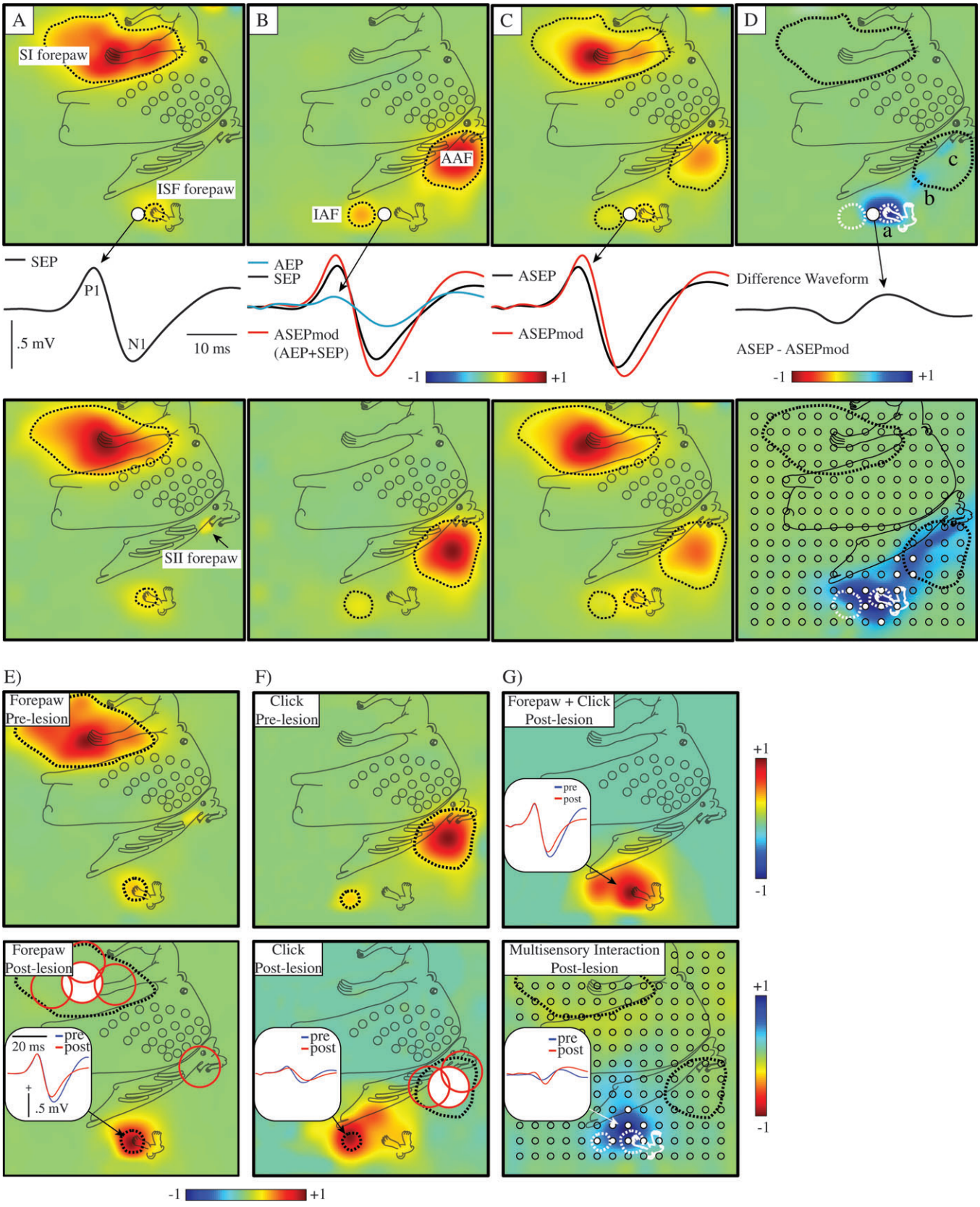
A
SI forepaw
ISF forepaw
B
AAF
IAF
C
D
c
b
a
SEP
P1
N1
.5 mV
10 ms
AEP
SEP
ASEPmod
(AEP+SEP)
-1
+1
ASEP
ASEPmod
Difference Waveform
ASEP - ASEPmod
-1
+1
SII forepaw
E)
Forepaw
Pre-lesion
F)
Click
Pre-lesion
G)
Forepaw + Click
Post-lesion
pre
post
+1
-1
Forepaw
Post-lesion
20 ms
pre
post
+
.5 mV
Click
Post-lesion
pre
post
Multisensory Interaction
Post-lesion
pre
post
+1
-1
-1
+1

inhibitory interactions between the auditory and somatosensory responsive cells.

Figure 2 (top maps) show a single animal's response to forepaw, auditory, and combined stimulation. Figure 2*A* (top map) shows this animal's forepaw representations in both SI and ISF (note again that the forepaw response in SII was smaller at the chosen P1 latency than ISF and therefore attenuated in this map normalized to the much larger SI responses). The SEP from an electrode site just rostral to the center of the ISF forepaw representation and caudal to IAF (Fig. 2*A*; top map; large white dot) is enlarged (Fig. 2*A*; middle black trace). Responses in AAF and the IAF are mapped in Figure 2*B* (top map), with enlargement of the AEP from the same electrode site caudal to IAF (Fig. 2*B*; middle blue trace). Superimposed on the enlarged AEP is the previously depicted SEP (black trace) for comparison. When these unimodal AEP and SEP waveforms were added, they comprised a linear model (Fig. 2B; ASEPmod; red trace). Simultaneous combined forepaw and auditory stimulation resulted in activation of IAF and AAF as well as the forepaw representation of SI and ISF (Fig. 2*C*; top map). The enlarged ASEP (Fig. 2*C*; middle black trace) was of both lower amplitude (subadditive) and shorter poststimulus latency than the previously computed ASEPmod (Fig. 2*C*; middle red trace), indicating that the multisensory response involved neuronal interaction between IAF and ISF. Subtraction of the ASEPmod from the ASEP resulted in a difference waveform (Fig. 2*D*; middle black trace) whose RMS power reflected the magnitude of nonlinearity or multisensory interaction. In this animal, the region of multisensory interaction partially overlapped the caudal border of IAF and the complete forepaw representation of ISF (Fig. 2*Da*; top map), as well as the intervening region between IAF and ISF. Note that here and in other maps of multisensory interaction, the color bar has been reversed so that positive RMS power is represented by a maximum blue region, providing contrast to other plots of the P1 (reflecting amplitude in mV as opposed to power). Two other areas of weaker multisensory interaction were also apparent caudal and medial to the insular site (Fig. 2*Db* and *c*) at the borders of AAF and corresponding to previously reported rostral and caudal multisensory zones in rat (Brett-Green et al. 2000, 2003, 2004; Menzel and Barth 2005). No multisensory responsiveness was detected in the forepaw representation of SI (Fig. 2*D*; top map; medial dashed outline) or the center of AAF (Fig. 2*D*; top map; caudal dashed outline).

Across animals ($N = 5$), the RMS power of the difference waveform, computed in this way, averaged 0.3 ± 0.02 mV. Much of the multisensory interaction was reflected in shorter poststimulus latencies of the multisensory response, shifted by 0.7 ± 0.02 ms earlier ($P < 0.01$; $N = 5$). The P1 of the ASEP was also subadditive (ASEP = 0.5 ± 0.01 mV; ASEPmod = 0.8 ± 0.02 mV; $P < 0.04$; $N = 5$), and contributed to the difference waveform. Nonlinearities in the N1 did not reach significance across animals ($P = 0.35$; $N = 5$). The bottom row of maps in Figure 2 depicts response patterns similar to the single animal described above but averaged across 5 animals. The averaged SEP (Fig. 2*A*; bottom map) corresponded closely with the single animal response shown in the top map with the exception that a weak response in the forepaw region of SII (arrow) could also be discerned. Averaged responses for the AEP (Fig. 2*B*; bottom map) and ASEP (Fig. 2*C*; bottom map) also corresponded closely to the single animal examples above. However, the region of multisensory interaction was more extensive in the grand average (Fig. 2*D*; bottom map), covering much of IAF, ISF, and intervening cortex, and extending approximately 1 mm medial and 0.5 mm lateral to these loci. Multisensory interactions were also more prominent in the rostral and caudal multisensory zones at the borders of AAF. To assess the spatial distribution of significant multisensory interactions across animals, we compared RMS power of the 25 ms prestimulus baseline to the 25 ms poststimulus response period of the difference waveform computed at each electrode site, using *t*-tests set to a significance of $P < 0.05$. Electrode sites displaying significant interactions (Fig. 2*D*; bottom map; filled white circles) where located in caudal IAF, rostral ISF, and several intervening sites. Sites located in the rostral but not the medial multisensory zones of AAF also reached significance. Again, no significant multisensory responses were noted in SI or the center of AAF.

Unisensory and Multisensory Processing in the Cortically Isolated Insula.

Observation that significant multisensory interactions occurred in the insula raised the question of whether the responses were dependent in part on recently established intracortical connections with AAF (Kimura et al. 2007). However, the fact that AEPs in the IAF had a shorter poststimulus latencies than those of AAF suggested that IAF may not rely solely on these intracortical projections for access to auditory input and that both unisensory and multisensory processing in the insula may occur in parallel and independent of input from other primary and secondary sensory regions. Figure 2 (*E,F*; top maps) shows an example of primary, secondary, and insular cortex responses to forepaw (*E*) and auditory (*F*) stimulation. The location and extent of radio frequency lesions (see Methods) were guided by hemispheric maps, such as these, for each animal. A lesion was 1st placed in the approximate center of primary cortex (white filled red circles in Fig. 2*E,F*; bottom maps). The recording array was then replaced and responses in the targeted region rechecked and used to guide the placement of subsequent lesions (empty red circles in Fig. 2*E,F*; bottom maps). As in this example, 3–4 lesions in the forepaw representation of SI, 1 lesion in the forepaw representation of SII and 2–3 lesions in AAF, spaced by approximately 1–2 mm, were required to completely eliminate evoked responses in primary and secondary auditory and somatosensory cortex.

Corresponding bottom plates of this figure indicate that destruction of the forelimb area of SI and SII, and responsive areas of AAF, left responses in IAF and ISF intact. Across the 5 animals lesioned, there were no significant differences in the locations of these areas pre- and postlesion. Although maps of the AEP and SEP appeared larger in amplitude and more widely distributed postlesion, this effect was due to normalization based on the largest response amplitudes in the array, which prelesion were dominated by large responses in primary cortex. Although pre- and postlesion SEP and AEP appeared to differ slightly in amplitude and morphology (Fig. 3*E,F*; bottom plates; inserts), these differences did not reach significance. Pre- and postlesion P1 amplitudes in the ISF forepaw representation were 0.8 ± 0.03 and 0.9 ± 0.05 mV ($P = 0.56$; $N = 5$), and N1 amplitudes were −1.2 ± 0.04 and −1.2 ± 0.1 mV ($P = 0.99$; $N = 5$), respectively. Similarly, in the IAF, pre- and postlesion P1 amplitudes were 0.4 ± 0.03 and 0.3 ± 0.04 mV ($P = 0.17$; $N = 5$), and N1 amplitudes were −0.7 ± 0.03 and −0.4 ± 0.07 mV ($P = 0.07$; $N = 5$), respectively. Nor were there any significant changes in component latencies introduced by

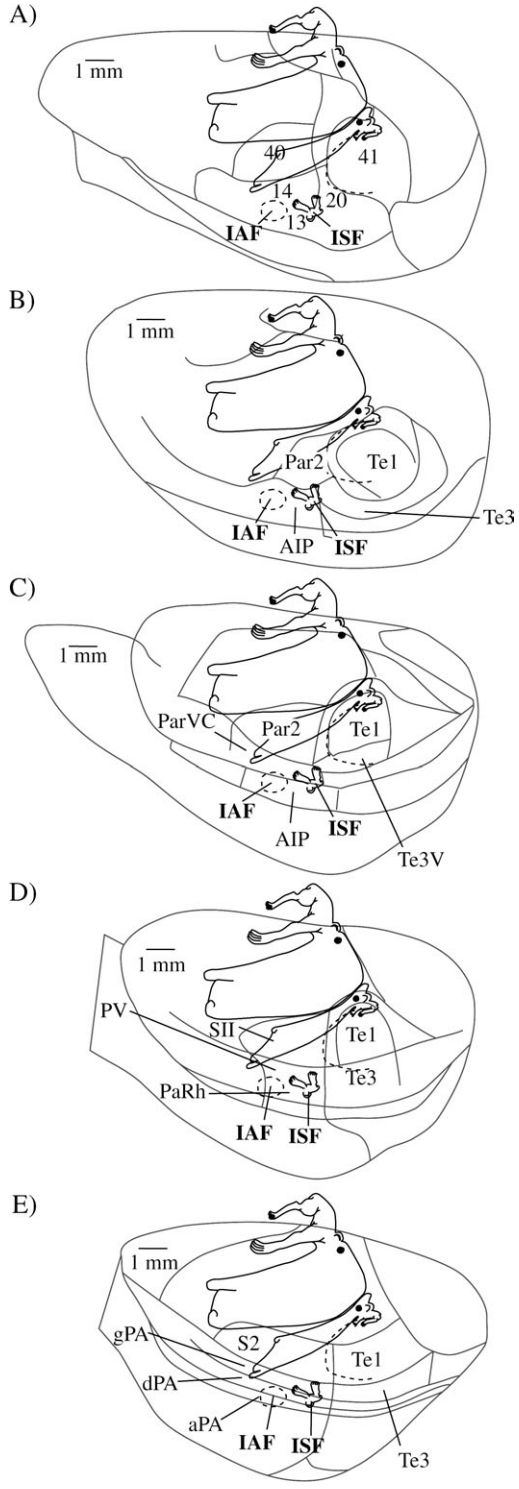

Figure 3. Relationship of IAF and ISF to areal maps of rat cortex. A ratunculas from the present study is superimposed onto areal maps from numerous investigators to show the approximate relationship of IAF and ISF to relevant areas. (*A*) Krieg (Krieg 1946). IAF and ISF fall rostral to Krieg's area 20 and lateral to area 40, centered within insular areas 13 and 14. (*B* and *C*) Flattened and unflattened hemispheres of Zilles and Wree and Palomero-Gallagher and Zilles, respectively (Palomero-Gallagher and Zilles 2004; Zilles and Wree 1985). Again IAF and ISF fall within insular cortex, specifically the agranular insular posterior area (AIP) just rostral to the auditory belt cortex (Te3) and lateral to secondary somatosensory cortex (Par2). In this and the remaining maps, primary auditory cortex is labeled "Te1." In the 2nd and more recent map of these workers (*C*) IAF and ISF are still placed in AIP, but now overlap another area, the ventral caudal part of parietal cortex (ParVC). (*D*) McDonald et al. (1999). ISF is lateral to secondary somatosensory cortex (SII) and falls within the posterior insular cortex, mainly within the PV area. Most of IAF and ISF fall within the parietal rhinal cortex (PaRh). (*E*) Shi and Cassel, (Shi and Cassell 1998). Again, IAF and ISF are lateral to secondary somatosensory cortex (S2) and overlap the posterior insular cortex (defined as granular and dysgranular parietal insular cortex, gPA and dPA), as well as, the agranular parietal insular cortex (aPA).

lesioning primary cortex. Pre- and postlesion P1 latencies in ISF were 19.1 ± 0.01 and 19.2 ± 0.01 ms ($P = 0.61$; $N = 5$), and N1 latencies were 28.4 ± 0.03 and 28.0 ± 0.03 ms ($P = 0.69$; $N = 5$), respectively. In IAF, pre- and postlesion P1 latencies were 18.1 ± 0.02 and 18.6 ± 0.02 ms ($P = 0.42$; $N = 5$), and N1 latencies were 27.2 ± 0.03 and 29.1 ± 0.04 ms ($P = 0.12$; $N = 5$), respectively.

Multisensory interactions also persisted unaltered following cortical isolation. Similar to unisensory responses, multisensory responses were unaffected by lesioning (Fig. 2*G*; top map) and appeared to rely on thalamocortical afferents. The RMS power of multisensory interaction in these animals was 0.32 ± 0.02 and 0.31 ± 0.02 mV ($P = 0.45$; $N = 5$) before and after lesioning, respectively (Fig. 2*G*; bottom map). The postlesion multisensory map of Figure 2*G* is representative of a single animal. Yet, electrode sites displaying significant interactions across animals ($N = 5$) were similar to the prelesion response pattern of Figure 2*D* (bottom map). Significant multisensory responses were recorded in IAF, the forepaw representation of ISF, intervening cortex between IAF and ISF, as well as regions extending 1 mm medial to this locus (Fig. 2*G*; bottom plate; white dots). As might be expected, multisensory interactions in all areas of AAF were eliminated.

Discussion

The present results demonstrate distinct auditory, somatosensory, and multisensory regions in the posterior insula of the rat. Whole-hemisphere mapping indicates that these areas are distinguishable from primary and secondary auditory and somatosensory cortex, and appear to rely predominately on thalamocortical afferent input.

Relationship of IAF and ISF to Areal Maps of Rat Cortex

A number of investigators have presented areal maps of rat cortex, with intraareal borders defined principally by cytoarchitectural boundaries and existing functional mapping (Krieg 1946; Zilles and Wree 1985; Shi and Cassell 1998; McDonald et al. 1999; Palomero-Gallagher and Zilles 2004). The earliest still cited areal map is that by Kreig (1946), and has been adapted in Figure 3*A* with a superimposed ratunculus from the present study to show the approximate relationship of IAF and ISF to relevant areas. In this, and subsequent plates of this figure, every attempt was made to equalize the scales of areal maps for comparison and to scale and orient our ratunculus based on locations of the rhinal fissure and other structural and functional landmarks, most prominently, primary auditory, somatosensory and visual cortex, because these were well defined in our functional mapping as well as in the areal maps. However, spatial relationships must be regarded as approximate because scales were not provided in any publications. By this method, the locations of ISF and IAF may be compared with delineations of insular cortex provided by Krieg (1946; Fig. 3*A*), Zilles and colleagues (Zilles and Wree 1985; Palomero-Gallagher and Zilles 2004; Fig. 3*B*,*C*), McDonald et al. (1999;

Fig. 3*D*), and Shi and Cassell (1998; Fig. 3*E*). Despite the variations in terminology and areal boundaries used by these workers, comparison to areal studies of rat cortex to date places IAF and ISF just rostral to secondary auditory cortex (variously termed Area 20 and Te3) and lateral to secondary somatosensory cortex (variously termed Area 40, Par2, SII, and S2). Representation of the distal extremities of ISF lay in the dorsal part of posterior insular cortex (variously termed Area 14, AIP, ParVC, PV, and gPA), whereas the trunk representation of ISF and all of IAF lay in the ventral part of posterior insular cortex (variously termed Area 13, AIP, PaRh, dPA, and aPA).

Somatosensory Responses of the Insula

Anterior insular cortex, between bregma levels +2.5 and –1.0, is generally considered to be involved in gustatory and visceral functions (Kosar et al. 1986a, 1986b; Cechetto and Saper 1987; Fabri and Burton 1991a, 1991b; Shi and Cassell 1997; McDonald 1998; McDonald et al. 1999). However, the remaining posterior insular cortex, between bregma levels –1.0 and –3.5, is thought to be involved in somesthesis and thus has been referred to as the somatosensory insula (Ito 1998; McDonald 1998; Shi and Cassell 1998; McDonald et al. 1999). Recent microelectrode (Remple et al. 2003) and field potential (Benison et al. 2007) studies in the rat confirm the somatosensory responsiveness of this region (referred to in these papers as PV) and have indicated a detailed somatotopic organization similar to the present ISF, forming an inverted and rostrally oriented ratunculus. It has been proposed that the somatosensory PV described for the rat (Fabri and Burton 1991a; Remple et al. 2003) is analogous to PV in other mammals, including monkeys and humans (Disbrow et al. 2000). However, although somesthetic responsiveness of the posterior insula has been reported in a number of species (Sudakov et al. 1971; Robinson and Burton 1980a, 1980b; Mufson and Mesulam 1982; Flynn 1999), the correspondence of these insular areas with putative PV across species is inconsistent. Our functional maps fall well within the insula as defined by numerous areal parcellations of rat cortex (Krieg 1946; Zilles and Wree 1985; Shi and Cassell 1998; McDonald et al. 1999; Palomero-Gallagher and Zilles 2004), with the exception of McDonald et al. (1999) who refers to this area as PV. To remain consistent with most previous literature on rat insula that includes detailed cytoarchitectural and hodological analysis of this region, and because the ISF appears to be part of a single functional system including the IAF which extends to the rhinal vein, we refer to this region as ISF as opposed to PV, with the understanding that they may finally be equivalent in the rat.

Somatosensory functions of rat posterior insula may be deduced from projections to (Guldin and Markowitsch 1983; Fabri and Burton 1991a; Paperna and Makach 1991; McIntyre et al. 1996) and from (Akers and Killackey 1978; Guldin and Markowitsch 1983) SI and SII. The abundance of intracortical connections between SI and ISF may be indicative of a scheme involving sequential or hierarchical flow of somatosensory information from primary to secondary regions, as suggested from studies of primates. Indeed, the insular cortex has classically been regarded as lacking input from the thalamus, relying instead on intracortical afferent input (Paperna and Makach 1991). However, our results indicate the ISF has powerful parallel access to somatosensory information from the thalamus; complete lesioning of SI and SII has almost no effect on evoked responses in the ISF, at least in the present anesthetized animals. The most likely source of thalamic somatosensory input to the ISF is the ventrobasal, posterior, and parvocellular part of the ventroposterior lateral nuclei of the thalamus, as demonstrated by retrograde label injections into this region (Guldin and Markowitsch 1983; Shi and Cassell 1998).

Auditory Responses of the Insula

Despite evidence for involvement of the insula in auditory processing in other species (Bamiou et al. 2003), to our knowledge, the present recordings from IAF are the 1st evidence for distinct auditory processing in the rat insula. Microelectrode and optical imaging studies in the rat (Polley et al. 2007) have identified 4 distinct auditory fields that surround primary auditory cortex. The most anterior border of these fields (AAF) is positioned at bregma –3.0 mm (see Fig. 1*A* of Polley et al. 2007), corresponding closely with the anterior border of AAF in the present study (Fig. 1*B*) and approximately 2 mm caudal and 1 mm medial to the IAF (Kimura et al. 2007).

IAF may access auditory information via both intracortical and parallel thalamic pathways. Injection of anterograde tracer into the rostral border of AAF results in discrete labeling from bregma –0.7 to –2.1 mm (Kimura et al. 2007). This is quite close to the locus and extent of IAF (bregma –0.5 to –1.5). In an earlier study (Paperna and Makach 1991), anterograde tracer injections into AAF labeled cells in a region that clearly overlaps the IAF. Injection of retrograde tracer into the center of the caudal part of granular insular cortex (corresponding approximately to IAF) labels cells in primary auditory cortex as well as the medial division of the MG nucleus and suprageniculate nucleus of the thalamus (Guldin and Markowitsch 1983). Injections of retrograde tracer into the center of the caudal part of the granular insular cortex (Krettek and Price 1977), close to IAF, results in labeling of the internal division of the MG nucleus and suprageniculate nucleus, providing a direct thalamocortical auditory afferent projection to the IAF. Again, our data indicate that lesioning of all primary and secondary auditory fields, sufficient to completely eliminate the AEP in temporal cortex, has no significant effect on the latency, amplitude, or morphology of responses in the IAF, suggesting that the dominant source of auditory input to this area is thalamic as opposed to cortical.

Multisensory Responses of the Insula

The intracortical and thalamocortical connectivity of posterior insula has prompted some (Guldin and Markowitsch 1983) to term this area "associative insular cortex," anticipating its multisensory function. Overlapping responses from IAF and ISF could be produced by interdigitated auditory and somatosensory responsive cells and/or volume conducted field potentials from otherwise separate auditory and somatosensory fields. However, multisensory stimulation consistently evokes responses that are of earlier poststimulus latency and lower amplitude than the summed AEP and SEP, both hallmarks of multisensory integration (Dehner et al. 2004; Rowland et al. 2007; Stanford and Stein 2007). Although these results demonstrate a clear multisensory responsiveness within the insula, and quantify its spatial and temporal properties under limited stimulus conditions (click and forepaw stimulation),

this subject deserves more elaboration than provided here. Of particular interest will be future work to establish whether individual cells in multisensory insula are sensitive to concordant spatial tuning as demonstrated in other areas of multisensory cortex and the superior colliculus (Stein and Meredith 1993).

Several studies have identified somatosensory/auditory responses in regions of secondary auditory cortex of rats (Brett-Green et al. 2004; Menzel and Barth 2005), squirrels (Krubitzer et al. 1986), monkeys (Schroeder et al. 2001; Schroeder and Foxe 2002), and humans (Foxe et al. 2001; Lütkenhöner et al. 2002; Murray et al. 2005). However, similar to unisensory auditory and somatosensory responses in the IAF and ISF, nonlinear multisensory insular responses are not significantly affected by complete ablation of these more caudal and medial multisensory zones along with primary and secondary auditory cortex and relevant areas of primary and secondary somatosensory cortex, indicating that integration is dominated by thalamocortical projections directly to the insula. The region of multisensory responsiveness overlaps caudal IAF, rostral ISF, and intervening cortex, suggesting that the integration observed here may be due at least in part to intracortical interactions between these areas. However, convergence of unisensory thalamocortical projections onto common cells within insular cortex may also contribute to unique multisensory responses. This possibility is consistent with demonstration that the posterior insula receives projections from the MG (Krettek and Price 1977; Guldin and Markowitsch 1983) and the ventrobasal and posterior region of the thalamus (Guldin and Markowitsch 1983; Shi and Cassell 1998). It is notable that much of the thalamic projection to the insular cortex is from the medial division of the MG, suprageniculate, and posterior nuclei, which are themselves known to be multisensory areas of the thalamus (Winer and Morest 1983; Steriade et al. 1997; Brett-Green et al. 2003), suggesting that multisensory insular responses may also reflect integration already effected at the thalamic level.

Functional Implications

Although the posterior insular cortex in several species has been suspected to be involved in multisensory integration (Loe and Benevento 1969; Benevento et al. 1977; Robinson and Burton 1980a, 1980b; Wehr and Laurent 1996; Flynn 1999), little else is known about the putative function of this region. One intriguing possibility is that this area is distinctly involved in fear conditioning, as proposed by others based on lesioning studies (Campeau and Davis 1995; Brunzell and Kim 2001; Lanuza et al. 2004). Interestingly, fear conditioning experiments in rats typically involve pairing of an innocuous auditory conditioned stimulus with a noxious somatosensory unconditioned stimulus such as foot shock, similar to the stimulus paradigm of the present study. The possibility that multisensory integration in the IAF and ISF may contribute to such fear conditioning is consistent with studies suggesting that the posterior insula may be especially sensitive to noxious somatosensory stimuli (Flynn 1999; Frot et al. 2007). The large cutaneous stimulating currents (1.0–2.0 mA) required in the present study to evoke reliable responses in ISF exceed the 0.5 mA typically used for foot shock in fear conditioning studies (Lanuza et al. 2004). Although it is possible to activate cells in this region with innocuous mechanical stimulation (Remple et al. 2003), our field potential measures, which reflect the central tendency of the entire population, suggest a predominant requirement for strong and possibly noxious stimulation levels (also noted earlier by Ito 1998). As noted in the Methods section, when currents of 1.0–2.0 mA are applied to the paws of unanesthetized rats, they result in vigorous withdrawal reflexes suggestive of noxious stimulation. Yet, such strong currents do not only activate nociceptors and do not exclusively indicate a preference of the ISF for noxious as opposed to simply strong stimulation. Another link between the ISF and IAF and fear conditioning comes from histological tracer studies demonstrating efferent projections from the posterior insula to the amygdala (McDonald 1998; Shi and Cassell 1998), a structure that is thought to be essential for affective processing underlying fear conditioned responses (LeDoux and Farb 1991). Interestingly, although a number of previous studies (Mascagni et al. 1993; Romanski and LeDoux 1993; Shi and Cassell 1997), have suggested that a ventral auditory area (VA) at the juncture between Te1 and Te3 may serve as a key link in fear conditioning, bringing auditory information to the amygdala, it has very recently been demonstrated with Biocytin injections (Kimura et al. 2007) that the VA does not project to the amygdala, but instead, to a well defined area of posterior insula corresponding almost exactly with the location of IAF. Thus, the IAF and ISF may serve as the source of innocuous auditory and noxious somatosensory afferent input to the amygdala, respectively. The present methods, permitting precise lesioning of the ISF and IAF based on high-resolution functional mapping, should provide a useful tool for evaluating the possible role of these regions in fear conditioning paradigms in future studies.

Funding

National Institutes of Health (NS36981); University of Colorado Council for Research and Creative Work; and University of Colorado Undergraduate Research Opportunity Program.

Notes

Conflict of Interest: None declared.

Address correspondence to Daniel S. Barth, Ph.D. Department of Psychology, University of Colorado, Campus Box 345, Boulder, CO 80309-0345, USA. Email: dbarth@psych.colorado.edu.

References

Akers RM, Killackey HP. 1978. Organization of corticocortical connections in the parietal cortex of the rat. J Comp Neurol. 181: 513–538.

Aleksandrov VG, Fedorova KP. 2003. Structure of the insular region of the rat neocortex. Neurosci Behav Physiol. 33:199–202.

Bamiou DE, Musiek FE, Luxon LM. 2003. The insula (Island of Reil) and its role in auditory processing. Literature review. Brain Res Brain Res Rev. 42:143–154.

Benevento LA, Fallon J, Davis BJ, Rezak M. 1977. Auditory-visual interaction in single cells in the cortex of the superior temporal sulcus and the orbital frontal cortex of the macaque monkey. Exp Neurol. 57:849–872.

Benison AM, Rector DM, Barth DS. 2007. Hemispheric mapping of secondary somatosensory cortex in the rat. J Neurophysiol. 97: 200–207.

Brett-Green B, Fifkova E, Larue D, Winer J, Barth DS. 2003. A multimodal zone in rat parieto-temporal cortex: intra- and extracellular

physiology and thalamocortical connections. J Comp Neurol. 460:223–237.
Brett-Green B, Paulsen M, Staba RJ, Fifkova E, Barth DS. 2004. Two distinct regions of secondary somatosensory cortex in the rat: topographical organization and multisensory responses. J Neurophysiol. 91:1327–1336.
Brett-Green B, Walsh K, Barth DS. 2000. Polysensory cortex in the rat: field potential mapping and intracellular recording. Soc Neurosci Abs. 26:1976.
Brunzell DH, Kim JJ. 2001. Fear conditioning to tone, but not to context, is attenuated by lesions of the insular cortex and posterior extension of the intralaminar complex in rats. Behav Neurosci. 115:365–375.
Burton H, Jones EG. 1976. The posterior thalamic region and its cortical projection in New World and Old World monkeys. J Comp Neurol. 168:249–301.
Campeau S, Davis M. 1995. Involvement of subcortical and cortical afferents to the lateral nucleus of the amygdala in fear conditioning measured with fear-potentiated startle in rats trained concurrently with auditory and visual conditioned stimuli. J Neurosci. 15: 2312–2327.
Cechetto DF, Saper CB. 1987. Evidence for a viscerotopic sensory representation in the cortex and thalamus in the rat. J Comp Neurol. 262:27–45.
Deacon TW, Eichenbaum H, Rosenberg P, Eckmann KW. 1983. Afferent connections of the perirhinal cortex in the rat. J Comp Neurol. 220:168–190.
Dehner LR, Keniston LP, Clemo HR, Meredith MA. 2004. Cross-modal circuitry between auditory and somatosensory areas of the cat anterior ectosylvian sulcal cortex: a 'new' inhibitory form of multisensory convergence. Cereb Cortex. 14:387–403.
Disbrow E, Roberts T, Krubitzer LA. 2000. Somatotopic organization of cortical fields in the lateral sulcus of Homo sapiens: evidence for SII and PV. J Comp Neurol. 418:1–21.
Downar J, Crawley AP, Mikulis DJ, Davis KD. 2000. A multimodal cortical network for the detection of changes in the sensory environment. Nat Neurosci. 3:277–283.
Fabri M, Burton H. 1991a. Ipsilateral cortical connections of primary somatic sensory cortex in rats. J Comp Neurol. 311:405–424.
Fabri M, Burton H. 1991b. Topography of connections between primary somatosensory cortex and posterior complex in rat: a multiple fluorescent tracer study. Brain Res. 538:351–357.
Flynn FG. 1999. Anatomy of the insula functional and clinical correlates. Aphasiology. 13:55–78.
Foxe JJ, Wylie GR, Martinez A, Schroeder CE, Javitt DC, Guilfoyle D, Ritter W, Murray MM. 2001. Auditory-somatosensory multisensory processing in auditory association cortex: an fMRI study. J Neurophysiol. 88:540–543.
Frot M, Magnin M, Mauguiere F, Garcia-Larrea L. 2007. Human SII and posterior insula differently encode thermal laser stimuli. Cereb Cortex. 17:610–620.
Guldin WO, Markowitsch HJ. 1983. Cortical and thalamic afferent connections of the insular and adjacent cortex of the rat. J Comp Neurol. 215:135–153.
Ito SI. 1998. Possible representation of somatic pain in the rat insular visceral sensory cortex: a field potential study. Neurosci Lett. 241: 171–174.
Kimura A, Donishi T, Okamoto K, Imbe H, Tamai Y. 2007. Efferent connections of the ventral auditory area in the rat cortex: implications for auditory processing related to emotion. Eur J Neurosci. 25:2819–2834.
Kosar E, Grill HJ, Norgren R. 1986a. Gustatory cortex in the rat. I. Physiological properties and cytoarchitecture. Brain Res. 379: 329–341.
Kosar E, Grill HJ, Norgren R. 1986b. Gustatory cortex in the rat. II. Thalamocortical projections. Brain Res. 379:342–352.
Krettek JE, Price JL. 1977. The cortical projections of the mediodorsal nucleus and adjacent thalamic nuclei in the rat. J Comp Neurol. 171:157–191.
Krieg WJS. 1946. Connections of the cerebral cortex I. The albino rat. A) Topography of the cortical areas. J Comp Neurol. 84:221–275.
Krubitzer LA, Sesma MA, Kaas JH. 1986. Microelectrode maps, myloarchitecture, and cortical connections of three somatotopically organized representations of the body surface in the parietal cortex of squirrels. J Comp Neurol. 250:403–430.
Lanuza E, Nader K, Ledoux JE. 2004. Unconditioned stimulus pathways to the amygdala: effects of posterior thalamic and cortical lesions on fear conditioning. Neuroscience. 125:305–315.
LeDoux JE, Farb CR. 1991. Neurons of the acoustic thalamus that project to the amygdala contain glutamate. Neurosci Lett. 134: 145–149.
Loe PR, Benevento LA. 1969. Auditory-visual interaction in single units in the orbito-insular cortex of the cat. Electroencephalogr Clin Neurophysiol. 26:395–398.
Lütkenhöner B, Lammertmann C, Simões C, Hari R. 2002. Magnetoencephalographic correlates of audiotactile interaction. Neuroimage. 15:509–522.
Mascagni F, McDonald A, Coleman J. 1993. Corticoamygdaloid and corticocortical projections of the rat temporal cortex: a Phaseolus vulgaris leucoagglutinin study. Neuroscience. 57:697–715.
McDonald AJ. 1998. Cortical pathways to the mammalian amygdala. Prog Neurobiol. 55:257–332.
McDonald AJ, Shammah-Lagnado SJ, Shi C, Davis M. 1999. Cortical afferents to the extended amygdala. Ann N Y Acad Sci. 877:309–338.
McIntyre DC, Kelly ME, Staines WA. 1996. Efferent projections of the anterior perirhinal cortex in the rat. J Comp Neurol. 369: 302–318.
Menzel RR, Barth DS. 2005. Multisensory and secondary somatosensory cortex in the rat. Cereb Cortex. 15:1690–1696.
Mesulam MM, Mufson EJ. 1985. The insula of Reil in man and monkey. Architectonics, connectiivity, and function. In: Jones EG, Peters A, editors. Cerebral cortex. New York: Plenum Press. p. 179–226.
Mufson EJ, Mesulam MM. 1982. Insula of the old world monkey. II: Afferent cortical input and comments on the claustrum. J Comp Neurol. 212:23–37.
Murray MM, Molholm S, Michel CM, Heslenfeld DJ, Ritter W, Javitt DC, Schroeder CE, Foxe JJ. 2005. Grabbing your ear: rapid auditory-somatosensory multisensory interactions in low-level sensory cortices are not constrained by stimulus alignment. Cereb Cortex. 15:963–974.
Palomero-Gallagher N, Zilles K. 2004. Isocortex. In: Paxinos G, editor. The rat nervous system. San Diego: Elsevier Academic Press. p. 729–757.
Paperna T, Makach R. 1991. Patterns of sensory intermodality relationships in the cerebral cortex of the rat. J Comp Neurol. 308: 432–456.
Polley DB, Read HL, Storace DA, Merzenich MM. 2007. Multiparametric auditory receptive field organization across five cortical fields in the albino rat. J Neurophysiol. 97:3621–3638.
Remple MS, Henry EC, Catania KC. 2003. Organization of somatosensory cortex in the laboratory rat (Rattus norvegicus): evidence for two lateral areas joined at the representation of the teeth. J Comp Neurol. 467:105–118.
Robinson CJ, Burton H. 1980a. Organization of somatosensory receptive fields in cortical areas 7b, retroinsula, postauditory and granular insula of M. fascicularis. J Comp Neurol. 192: 69–92.
Robinson CJ, Burton H. 1980b. Somatic submodality distribution within the second somatosensory (SII), 7b, retroinsular, postauditory, and granular insular cortical areas of M. fascicularis. J Comp Neurol. 192:93–108.
Rodgers KM, Benison AM, Barth DS. 2006. Two dimensional coincidence detection in the vibrissa/barrel field. J Neurophysiol. 96:1981–1990.
Romanski L, LeDoux J. 1993. Information cascade from primary auditory cortex to the amygdala: corticocortical and corticoamygdaloid projections of temporal cortex in the rat. Cereb Cortex. 3:515–532.
Rowland BA, Quessy S, Stanford TR, Stein BE. 2007. Multisensory integration shortens physiological response latencies. J Neurosci. 27:5879–5884.

Schroeder CE, Foxe JJ. 2002. The timing and laminar profile of converging inputs to multisensory areas of the macaque neocortex. Cogn Brain Res. 14:187–198.
Schroeder CE, Lindsley RW, Specht C, Marcovici A, Smiley JF, Javitt DC. 2001. Somatosensory input to auditory association cortex in the macaque monkey. J Neurophysiol. 85:1322–1327.
Shi C, Cassell M. 1997. Cortical, thalamic, and amygdaloid projections of rat temporal cortex. J Comp Neurol. 382:153–175.
Shi CJ, Cassell MD. 1998. Cascade projections from somatosensory cortex to the rat basolateral amygdala via the parietal insular cortex. J Comp Neurol. 399:469–491.
Stanford TR, Stein BE. 2007. Superadditivity in multisensory integration: putting the computation in context. Neuroreport. 18: 787–792.
Stein BE, Meredith MA. 1993. The merging of the senses. Cambridge, London: The MIT Press.
Steriade M, Jones EG, McCormick DA. 1997. Thalamus. Amsterdam: Elsevier.
Sudakov K, MacLean PD, Reeves A, Marino R. 1971. Unit study of exteroceptive inputs to claustrocortex in awake, sitting, squirrel monkey. Brain Res. 28:19–34.
Wehr M, Laurent G. 1996. Odour encording by temporal sequences of firing in oscillating neural assemblies. Nature. 384:162–165.
Winer JA, Morest DK. 1983. The medial division of the medial geniculate body of the cat: implications for thalamic organization. J Neurosci. 3:2629–2651.
Zilles K, Wree A. 1985. Cortex: areal and laminar structure. In: Paxinos G, editor. The rat nervous system. New York: Academic Press. p. 375–392.